



Contents lists available at ScienceDirect

## Quaternary Science Reviews

journal homepage: [www.elsevier.com/locate/quascirev](http://www.elsevier.com/locate/quascirev)

## Biomarker records of phytoplankton productivity and community structure changes in the Japan Sea over the last 166 kyr

Lei Xing<sup>a,b</sup>, Rongping Zhang<sup>a,b</sup>, Yanguang Liu<sup>c</sup>, Xiaochen Zhao<sup>a,b</sup>, Sumei Liu<sup>a</sup>, Xuefa Shi<sup>c</sup>, Meixun Zhao<sup>a,b,\*</sup>

<sup>a</sup>Key Laboratory of Marine Chemistry Theory and Technology, Ministry of Education, Ocean University of China, Qingdao 266100, China

<sup>b</sup>Institute of Marine Organic Geochemistry, Ocean University of China, Qingdao 266100, China

<sup>c</sup>Key Laboratory of Marine Sedimentology and Environmental Geology, State Oceanic Administration, First Institute of Oceanography, Qingdao 266061, China

### ARTICLE INFO

#### Article history:

Received 4 September 2010

Received in revised form

27 May 2011

Accepted 31 May 2011

Available online 18 July 2011

#### Keywords:

Japan Sea

Biomarker

Productivity

Community structure

### ABSTRACT

Glacial-interglacial sea level changes have caused drastic variations in the surface hydrography, ventilation and ecosystem structure in the Japan Sea. Previous reconstructions using microfossils and geochemical proxies suggested decreased productivity and a more calcareous plankton community during glacial periods. However, the inferred community structure change is not consistent with significantly lower salinity in the Japan Sea during the glacials, which would have had a deleterious effect on calcareous plankton growth. Here, biomarker records of ODP Site 797 are generated to further evaluate phytoplankton productivity and community structure changes in the Japan Sea over the last 166 kyr. Although the contents of the phytoplankton biomarkers changed by two to three orders of magnitude, there were no clear glacial-interglacial patterns as sediment biomarker contents reflected the combined effect of production and water column degradation. The collective assessments of our biomarker records and published records support previous conclusions of decreased productivity in the Japan Sea during the glacials. However, a community structure proxy based on the alkenone/brassicasterol ratio reveals a shift from a diatom-dominated community during the glacials to a coccolithophorid-dominated community during the interglacials, mainly as a result of surface salinity variations in the Japan Sea controlled by sea-level changes. Previous community structure reconstruction using biogenic carbonate/silica ratio could have been complicated by the different environmental factors governing silica and CaCO<sub>3</sub> dissolution in the Japan Sea.

© 2011 Elsevier Ltd. All rights reserved.

### 1. Introduction

The Japan Sea (JS) is a semi-enclosed marginal sea bounded by the Islands of Japan, the Korean Peninsula, and the Russian Far East (Fig. 1). It is connected to the North Pacific Ocean and the Okhotsk Sea through shallow and narrow straits (Tada et al., 2007). Among these straits, the Tsushima Strait and the Tsugaru Strait are the deepest with a maximum depth of approximately 130 m. The Tsushima Warm Current (TWC) is the main surface current flowing into the JS through the Tsushima Strait, and it flows out through the northern Tsugaru Strait and the Soya Strait (Fig. 1). As a branch of the Kuroshio Current, the TWC is characterized by high

temperature and salinity, but it is also influenced by the contribution of low-salinity East China Sea coastal water (ECSCW) which has higher nutrient concentrations. The TWC is the major source of nutrients in the modern JS, contributing 55% of phosphorous and 67% of nitrogen in the upper 200 m of the JS (Yanagi, 2002). Primary production in the JS is relatively high among marginal seas, ranging from 191 to 222 g C m<sup>-2</sup> year<sup>-1</sup> (Yamada et al., 2005).

Environmental changes during the glacial periods significantly changed the hydrography, productivity and community structure in the JS. Sea level fall during the glacials led to drastic decreases in the flux of the warm and saline TWC into the JS, but the inflow of low-salinity ECSCW could have increased due to the seaward migration of the coastline (Fig. 1) (Tada et al., 1999). Lower surface salinity during the glacial periods strengthened stratification, reduced deep water ventilation, and caused significant changes of productivity and planktonic community structure of the JS (Oba et al., 1991; Lee et al., 2003; Hyun et al., 2007; Khim et al., 2007; Kido et al., 2007). Biogenic silica (BSi) records of many cores from the JS have revealed

\* Corresponding author. Key Laboratory of Marine Chemistry Theory and Technology, Ministry of Education, Ocean University of China, Qingdao 266100, China. Tel./fax: +86 532 66782103.

E-mail address: [maxzhao@ouc.edu.cn](mailto:maxzhao@ouc.edu.cn) (M. Zhao).

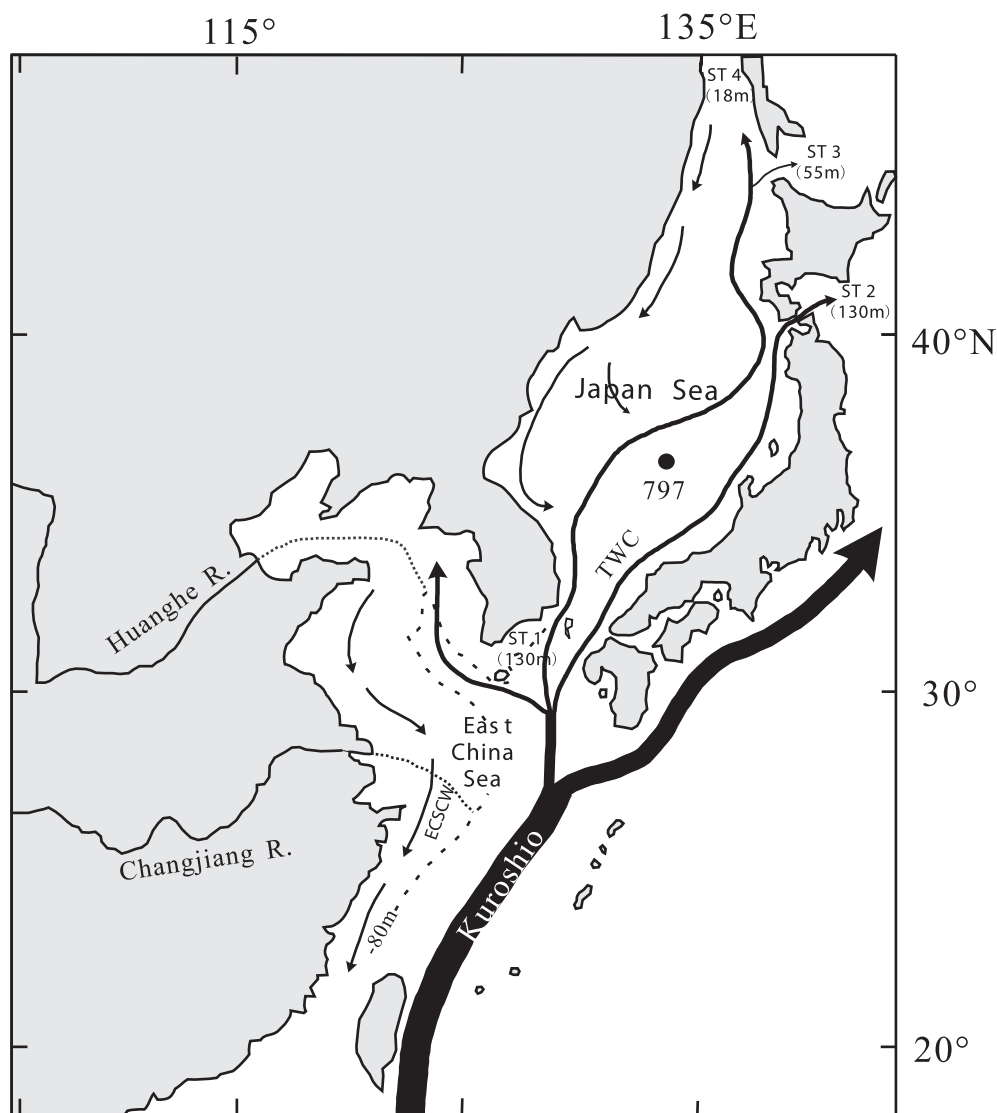


**Fig. 1.** ODP Site 797 (●) and the modern surface circulation (indicated by solid arrows) in the Japan Sea, East China Sea, and Yellow Sea. ECSCW represents the East China Sea Coastal Water. The dashed line indicates the bathymetric contour of 80 m in the East China Sea. Dotted lines represent the estimated paths of the Huanghe and Changjiang Rivers during glacial periods (Tada et al., 1999). ST 1 is the Tsushima Strait, ST 2 is the Tsugaru Strait, ST 3 is the Soya Strait and ST 4 is the Mamiya Strait.

a consistent pattern of higher values during the interglacials and lower values during the glacials (Oba et al., 1991; Gorbarenko, 1996; Hyun et al., 2007), suggesting higher productivity during interglacial periods. The BSi results were initially corroborated by measurements of total organic carbon (TOC) in sediments that also revealed generally higher values during the interglacials (Tada et al., 1999; Lee et al., 2003; Fujine et al., 2009). However, recent TOC studies from the JS have revealed some different patterns. In some cores, the TOC started to increase near the start of deglaciation at ca 15 ka instead of during the Holocene (Lee et al., 2003), while in ODP Site 797, the early intervals of interglacial MIS 5e and part of the Holocene were characterized by the lowest TOC content of the last 200 ka (Tada et al., 1999). Comparison of high resolution TOC record of ODP Site 797 with other proxies indicated that sedimentary TOC in the JS was mostly controlled by the redox state of the deep water. Thus, it was proposed that for the JS, TOC is not a reliable productivity indicator (Tada et al., 1999). The content of biogenic carbonate (BCa) in the JS generally showed higher values during the last glacial and lower values during the Holocene (Hyun et al., 2007). Carbonate variations in the JS were generally interpreted as reflecting both calcareous plankton surface production

and preservation efficiency (Hyun et al., 2007; Kido et al., 2007), thus, higher values during the last glacial could have been caused by either higher calcareous productivity or better preservation (Lee et al., 2003; Kido et al., 2007). Alkenone contents were low during the glacials, especially during the peak glacial intervals (Lee et al., 2008), indicating lower haptophyte (calcareous) productivity during glacials. Therefore, alkenone results provide some evidence that preservation rather than productivity is the main control on sedimentary carbonate content in the JS (Lee et al., 2003; Kido et al., 2007).

Phytoplankton community structure changes in the JS have been inferred mostly from the contrasting patterns of BCa and silica changes, with higher BCa content during the glacials and higher BSi content during the interglacials. These patterns were first revealed by Oba et al. (1991) in the Yamato Basin and by Gorbarenko (1996) in the Japan Basin, and were later confirmed by Hyun et al. (2007) who examined temporal variations in BSi and carbonate in six piston cores from the Tsushima Basin. The siliceous-carbonate mode switch was interpreted to have reflected major changes in the phytoplankton community structure from coccolithophore-dominant during the glacials to diatom-dominant during the

interglacials. It was suggested that these shifts were caused by changes in nutrient input (Hyun et al., 2007), however, the effect of salinity changes on phytoplankton community structure has not been evaluated. Salinity in the glacial JS was as much as 15 psu lower than it is today (Lee, 2007), which would not have favored the growth of calcareous planktons such as coccolithophores. Indeed, sediment alkenone content during the glacials was very low (Lee et al., 2008). Thus, alkenone records indicate that higher BCa contents during the glacial might not have been a result of community structure change, but most likely a result of better carbonate preservation due to a shallower CCD (Lee et al., 2000).

Hence, many questions remain concerning glacial-interglacial phytoplankton productivity and community structure changes in the JS, due to the combined influences of productivity and preservation on sedimentary BSi and carbonate contents. The multi-biomarker approach offers a means to reconstruct both productivity and community structure and this approach has the potential to circumvent some complications associated with preservation effects. As major components of phytoplankton cell membranes, lipid compounds such as sterols and alkenones are relatively well preserved in sediments, and their similar diagenetic properties support the use of biomarker ratios to reconstruct phytoplankton community structure changes (Schubert et al., 1998; Hinrichs et al., 1999). Recently, biomarkers have been successfully used to reconstruct glacial/interglacial changes in phytoplankton community structure from many regions (Schubert et al., 1998; Ishiwatari et al., 1999; Werne et al., 2000; Menzel et al., 2003; Schulte and Bard, 2003; Calvo et al., 2004; Dahl et al., 2004; Seki et al., 2004; Zhao et al., 2006; Xing et al., 2008). In this study, biomarkers from ODP Site 797 samples were analyzed in order (1) to reconstruct phytoplankton productivity and community structure changes of the JS over the last 166 kyr and (2) to evaluate how productivity and phytoplankton communities responded to nutrient and salinity changes over the last 166 kyr. The following biomarkers are used as proxies and indicators of phytoplankton productivity: brassicasterol for diatoms, dinosterol for dinoflagellates, alkenones ( $C_{37:2} + C_{37:3}$ ) for alkenone-producing coccolithophorid. Biomarker ratios are used as phytoplankton community structure proxies.

## 2. Material and methods

ODP Site 797 (38°36'58 N, 134°32'10 E, 2862 m water depth) was drilled in the south central part of the JS (Fig. 1). The site was not significantly influenced by turbidities which afforded continuous sediment deposition, and this was confirmed by the age model established by Tada et al. (1999). Several proxy records have been published for ODP Site 797, including BSi, BCa, TOC, and bottom water oxygen concentration (Tada et al., 1999; Irino and Tada, 2000, 2002).

194 samples were taken for biomarker analysis spanning the last 166 kyr with an average resolution of 0.85 kyr. Freeze-dried samples of about 2 g were extracted four times with a mixture of dichloromethane and methanol (3:1) by ultrasonication, after adding the  $C_{24}$  deuterium-substituted *n*-alkane and  $C_{19}$  alcohol as internal standards (IS). The total extracts were hydrolyzed in a KOH–MeOH solution and then separated into three fractions using silica gel chromatography. The neutral lipid fraction, which contains *n*-alkanols, alkenones and sterols, was dried and derivatized using *N*, *O*-bis (trimethylsilyl)-trifluoroacetamide (BSTFA) for instrumental analysis. Biomarker identification was performed on a Thermo gas chromatograph-mass spectrometer (GCMS), and quantification was performed on an Agilent 6890N GC, both using an HP-1 column (50 m). The content of each biomarker was calculated by ratioing its GC peak integration to that of the IS. Bulk

sediment flux is the product of LSR and DBD, where LSR is the linear sedimentation rate ( $\text{cm kyr}^{-1}$ ), and DBD is the dry bulk density ( $\text{g cm}^{-3}$ ). The mass accumulation rates (MARs) of the biomarkers were calculated by multiplying biomarker contents and bulk sediment flux. SST was calculated from the  $U_{37}^K$  index using the Müller equation,  $\text{SST} = (U_{37}^K - 0.044)/0.033$  (Müller et al., 1998).

## 3. Results and discussion

### 3.1. Content and MAR of biomarkers and phytoplankton productivity

Fig. 2 presents the records of biomarker content (dark lines) and MAR (red dashed lines), as well  $U_{37}^K$  SST and bulk sediment MAR, for the last 166 kyr.

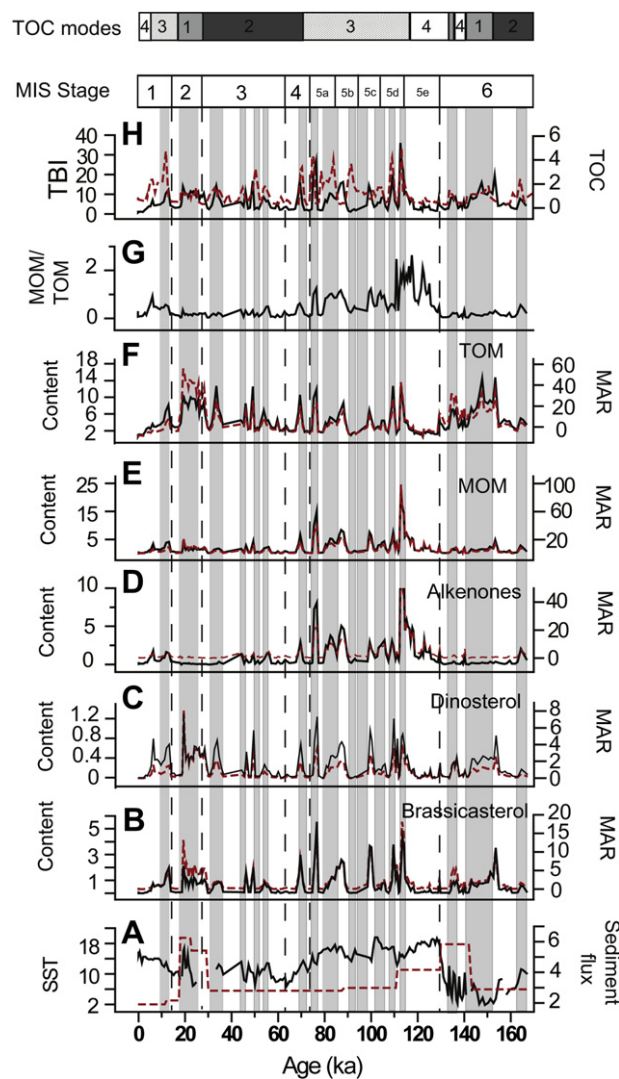


Fig. 2. Contents (solid lines) and mass accumulation rates (MARs, dashed lines) of biomarkers, and other proxy records for ODP Site 797. (A)  $U_{37}^K$  SST (solid line) ( $^{\circ}\text{C}$ ) and bulk sediment influx (dashed line) ( $\text{g cm}^{-2} \text{ kyr}^{-1}$ ); (B) content ( $\mu\text{g g}^{-1}$ ) and MAR ( $\mu\text{g cm}^{-2} \text{ kyr}^{-1}$ ) of brassicasterol; (C) content ( $\mu\text{g g}^{-1}$ ) and MAR ( $\mu\text{g cm}^{-2} \text{ kyr}^{-1}$ ) of dinosterol; (D) content ( $\mu\text{g g}^{-1}$ ) and MAR ( $\mu\text{g cm}^{-2} \text{ kyr}^{-1}$ ) of  $C_{37}$  alkenones; (E) content ( $\mu\text{g g}^{-1}$ ) and MAR ( $\mu\text{g cm}^{-2} \text{ kyr}^{-1}$ ) of marine organic matter (MOM, the sum of brassicasterol, dinosterol and alkenones); (F) content ( $\mu\text{g g}^{-1}$ ) and MAR ( $\mu\text{g cm}^{-2} \text{ kyr}^{-1}$ ) of the terrestrial organic matter (TOM,  $C_{28} + C_{30} + C_{32}$  *n*-alkanols); (G) the ratio of MOM content to TOM content,  $\mu\text{g g}^{-1}$ , solid line) and TOC (%wt, dashed line). The shaded vertical bars indicate dark layers (Tada et al., 1999). Marine isotope stages (MIS) and the TOC modes (Tada et al., 1999) are labeled on the top panels.

$U_{37}^K$  SST (Fig. 2A) oscillated between 3.8 and 21.5 °C, with minimum values in MIS 6 and maximum values in MIS 5c and MIS 5e. The core-top  $U_{37}^K$  SST of 17.2 °C is close to the observed modern annual average SST (17.17 °C) for the region (Japan Oceanographic Data Center). The  $U_{37}^K$  SST values during the last glacial maximum (LGM, 23–18 ka) oscillated between 16 and 18.8 °C which were much higher than those for MIS 6, and were even higher than the Holocene values, generally in agreement with previous results (Ishiwatari et al., 2001; Fujine et al., 2006; Lee et al., 2008). Although warmer LGM SSTs were first interpreted to be caused by radiative equilibrium associated with the development of strong stratification due to low surface salinity in the JS (Ishiwatari et al., 2001), this mechanism has not been supported by additional studies. Firstly, published (Fujine et al., 2006; Lee et al., 2008) and our results all show that  $U_{37}^K$  SSTs during the penultimate glacial maximum (PGM, 145–135 ka) of MIS 6 were much lower than those for MIS 5. Because the surface hydrographic conditions during the LGM and the PGM were likely similar, the SST differences between the LGM and PGM do not agree with this proposed mechanism for the LGM SST anomaly. Secondly, SST records reconstructed using other proxies, such as those based on radiolarian and diatom assemblages, all suggest that the JS experienced a cooling during the LGM (Koizumi et al., 2006; Itaki et al., 2007). Furthermore, climate records in the East China Sea near the Tsushima Strait (Ijiri et al., 2005) and off the east coast of Japan (Ohkushi et al., 2003; Oba et al., 2006) also revealed colder temperatures during the LGM.

Other likely explanations for the LGM anomaly could be that very low alkenone content affected the accurate estimation of SST using the  $U_{37}^K$  index (Lee et al., 2008), or that much lower salinity affected the productivity of alkenone-producing coccolithophorid species and resulted in higher SST (Fujine et al., 2006). However, these two explanations are also not supported by the longer records covering the MIS 6 period, because alkenone content for MIS 6 was similar or only slightly higher than that for the LGM but the MIS 6 SST was much lower. Alternatively, different genotypes of haptophytes in MIS 6 and MIS 2 could have responded differently to lower salinity environments (Fujine et al., 2009). Thus, additional studies are still needed to evaluate the SST differences between the LGM and the PGM revealed by the  $U_{37}^K$  index.

During the last 166 kyr, the content of biomarkers changed by two to three orders of magnitude, with brassicasterol from 0.016 to 5.55  $\mu\text{g g}^{-1}$  (Fig. 2B), dinosterol from 0.019 to 1.3  $\mu\text{g g}^{-1}$  (Fig. 2C), and alkenones from 0.025 to 20.18  $\mu\text{g g}^{-1}$  (Fig. 2D). The total content of brassicasterol, dinosterol and alkenones is used as a proxy for marine organic matter (MOM, Fig. 2E) input, and it varied between 0.46 and 23.36  $\mu\text{g g}^{-1}$ . The content of *n*-alkanols ( $C_{28} + C_{30} + C_{32}$ ) is used as a proxy for terrestrial organic matter (TOM, Fig. 2F) input, and it varied between 0.57 and 17.5  $\mu\text{g g}^{-1}$ . The MOM/TOM ratio (Fig. 2G) varied from 0.03 to 2.64, by almost two orders of magnitude. Brassicasterol and dinosterol content records show similar trends, with peak values occurring during both the glacials (MIS 2 and MIS 6) and interglacials (MIS 5a–5d, and the early Holocene), thus, a clear glacial-interglacial pattern does not emerge. The variations of the alkenone content were similar to those of brassicasterol and dinosterol during MIS 5 and MIS 4; but the alkenone content during MIS 6 and MIS 2 were very low while brassicasterol and dinosterol contents revealed significant variations. Overall, alkenone content values during the glacials were lower than those during the interglacials, with very high peak values during MIS 5 (especially near the MIS 5d–5e boundary).

The input of terrestrial materials can significantly change sedimentary biomarker contents, and the dilution effect can be evaluated by comparing biomarker contents with their corresponding MARs (Fig. 2B–E). Although the bulk sediment flux varied considerably, biomarker contents and MARs show similar trends,

suggesting that biomarker content variations were not controlled by terrestrial material dilution.

Both TOC and biomarker content (and MARs) have been used to reconstruct surface productivity in the JS (Tada et al., 1999; Lee et al., 2003; Hyun et al., 2007; Fujine et al., 2009). Based on this approach, our alkenone record (Fig. 2D) indicates that average alkenone-producing coccolithophorid productivity was lower during the glacials and higher during the interglacials, and MIS 5 productivity was much higher than those of other intervals. This glacial-interglacial pattern is in agreement with previous results from the JS. For example, a shorter record showed very low alkenone content values during the last glacial, maximum values in the early Holocene, and lower values during the late Holocene (Lee et al., 2003); longer time series revealed that the alkenone content had very high values during MIS 5, relatively high values during MIS 1, and low values during MIS 2, 3, 4, 6 (Lee et al., 2008). Strictly, sedimentary alkenone content is a productivity proxy for alkenone-producing coccolithophorids and most are open ocean species such as *Emiliania huxleyi* (up to 80%), and *Gephyrocapsa oceanica*, especially in warm environments (Winter et al., 1994 and references herein). Salinity changes in the JS could result in changes in predominant alkenone-synthesizing species, especially the coastal species during glacials as sea level dropped and salinity decreased. However, previous results have revealed that the coccolithophorid assemblages in the JS were dominated by *E. huxleyi* and *G. oceanica* over the last 36 kyr, and the relative abundance of *E. huxleyi* was close to or more than 50% except for the intervals between 9–10 ka and 19–20 ka (Ishiwatari et al., 2001). Thus to some extent, sedimentary alkenone contents from this and previous studies are useful indicators to discuss coccolithophorid productivity changes, which were lower during glacials.

In contrast, our brassicasterol and dinosterol records (both content and MAR, Fig. 2B and C) reveal no clear glacial-interglacial patterns of diatom and dinoflagellate productivity changes. Brassicasterol can also be produced by other microalgae in addition to diatoms, such as haptophytes and cryptophytes (Volkman, 1986), so its use as a diatom proxy needs to be comparatively evaluated. Since the variation of brassicasterol content differed significantly from that of alkenones, coccolithophorids were not likely the main producers of brassicasterol in ODP Site 797 and sediment brassicasterol contents mostly reflect diatom productivity changes.

Comparison of the MOM (Fig. 2E) and TOC (Fig. 2H) records for ODP Site 797 reveals some similarities, with generally higher values for both proxies during the interglacials, especially during MIS 5. However, there are also obvious differences, for example by comparing the two interglacials, TOC values of MIS 1 are similar to those of MIS 5 while MOM values of MIS 1 are much lower than those of MIS 5. One reason for these differences is that TOC contains both marine and terrestrial organic matter. A total biomarker index (TBI, Fig. 2H, created simply by adding TOM and MOM) reveals more similarity with the TOC record, confirming that both MOM and TOM were important contributors to sediment TOC in the JS. However, MOM (Fig. 2E) and TOM (Fig. 2F) reveal different temporal patterns, with MOM generally higher during interglacials suggesting higher productivity and TOM generally higher during glacials suggesting higher terrestrial inputs. The MOM/TOM (Fig. 2G) ratio also reveals a glacial-interglacial pattern, as MIS 5 values were much higher than MIS 6 values, and MIS 1 values higher than MIS 2 values, consistent with increased productivity during the interglacials. However, sediment MOM content (Fig. 2E) is partially controlled by depositional environments, especially since MOM is more labile than TOM. In ODP Site 797, both the MOM content (Fig. 2E) and the MOM/TOM ratio (Fig. 2F) reveal higher values during the interglacials than the glacials. Thus, water column and sedimentary degradation processes were not the main control on MOM, otherwise, MOM

content and MOM/TOM ratio would be lower as the JS environment was more oxic (Fig. 4F) during the interglacials. Significant terrestrial organic matter input to the JS could limit the use of TOC as a productivity proxy, thus to some extent, the MOM record is a better productivity proxy for the JS.

Lower productivity during the glacials was most likely related to sea level drop, which resulted in the reduction of the cross sectional area of the strait and the reduction of the TWC and the ECSCW inflows, and thus reduced nutrient inputs (Tada et al., 1999; Yanagi, 2002). Furthermore, lower salinity and strengthened stratification led to a weaker convection in the JS, resulting in decreased nutrient inputs and lower productivity (Tada et al., 1999). On the other hand, relative nutrient inputs from rivers to Site 797 could have increased due to the proximity of rivers to Site 797 during glacials. However, the JS region was much drier during the glacials (Tada et al., 1999; Irino and Tada, 2002), and river discharges could not have increased significantly. These combined factors suggest that the causes of lower glacial productivity in the JS are complex, but the more likely cause was the much weaker convection which limited nutrient input from the deep basin. However, productivity alone can not

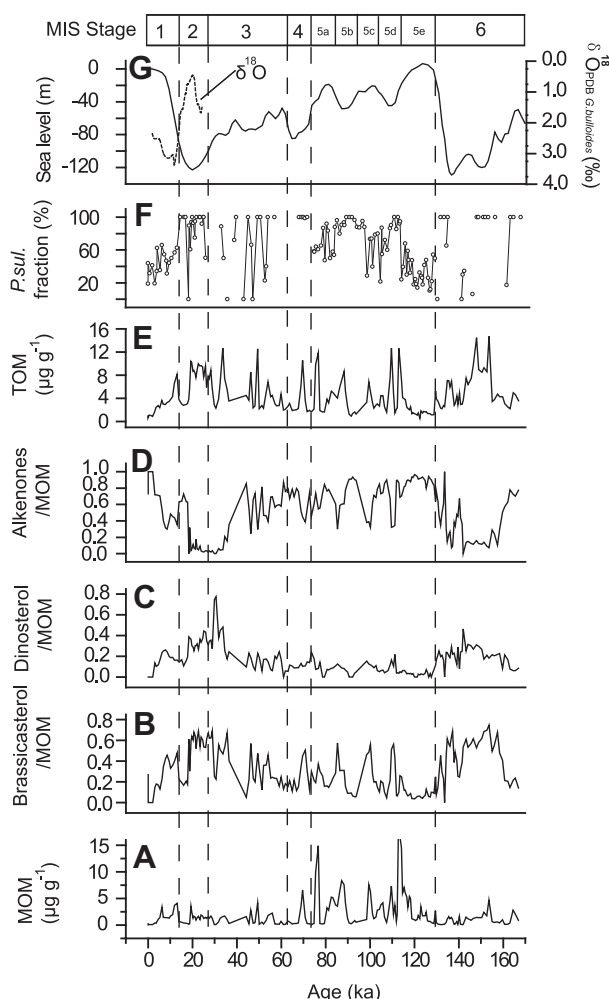


**Fig. 3.** Normalized (to the total content) biomarker contents for ODP Site 797. (A) marine organic matter (MOM) content ( $\mu\text{g g}^{-1}$ ); (B) normalized brassicasterol content; (C) normalized dinosterol content; (D) normalized alkenone content; (E) terrestrial organic matter (TOM) content ( $\mu\text{g g}^{-1}$ ), (F) *P. sulcata* fraction (%) and (G) Global sea level curve reconstructed using benthic foramineral  $\delta^{18}\text{O}$  (solid line; Waelbroeck et al., 2002) and the *Globigerina bulloides*  $\delta^{18}\text{O}$  record for the last 24 kyr of core TY99PC18 from the Japan Sea (dashed line; Lee, 2007). Marine isotope stages (MIS) are labeled on the top panel.

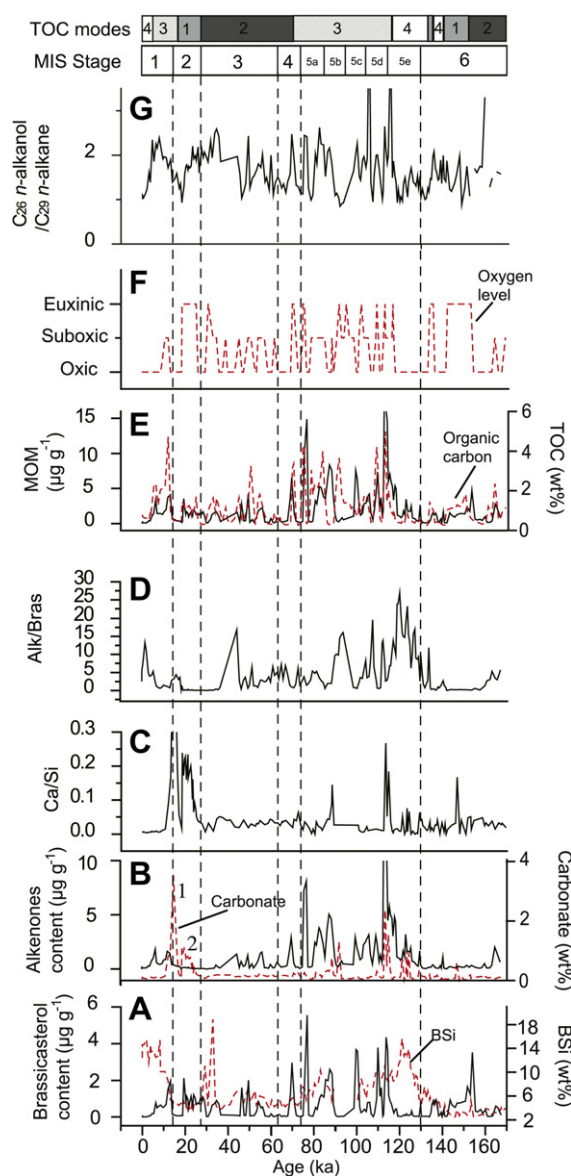


**Fig. 4.** Comparison of biomarkers and other proxies for ODP Site 797. (A) brassicasterol content ( $\mu\text{g g}^{-1}$ , solid line) and biogenic silica content (%wt, dashed line); (B)  $\text{C}_{37}$  alkenones content ( $\mu\text{g g}^{-1}$ , solid line) and biogenic carbonate (%wt, dashed line); (C) the ratio of biogenic carbonate (Ca) to biogenic silica (Si); (D) the ratio of  $\text{C}_{37}$  alkenones (alk) to brassicasterol (bras); (E) TOC (%wt, dashed line) and marine organic matter (MOM) content ( $\mu\text{g g}^{-1}$ , solid line); (F) bottom water oxygenation level (Tada et al., 1999); (G) the  $\text{C}_{26}$  n-alcohol/ $\text{C}_{29}$  n-alkane ratio. Marine isotope stages (MIS) and the TOC modes (Tada et al., 1999) are labeled on the top panels.

explain the detailed features of the biomarker records, especially on a millennial timescale. For example, biomarker contents for both MIS 5e and part of the Holocene were among the lowest (Fig. 2), even though the collective assessment of all evidence suggested higher productivity for these intervals.

For the JS, organic matter preservation efficiency has been an important factor controlling sediment organic content since bottom water redox conditions have changed significantly, especially on a millennial timescale (Tada et al., 1999). Quaternary hemipelagic sediments of the JS are characterized by centimeter- to decimeter-scale alterations of heavily bioturbated, organic-poor light layers and finely laminated, organic-rich dark layers. The organic contents in these layers have reflected changes in both productivity and bottom-water oxygenation with dark layers

during the glacials caused by better preservation of organic matter and dark layers during the interglacials caused by increased productivity (Tada et al., 1999; Watanabe et al., 2007; Yokoyama et al., 2007).

Comparison of our biomarker records and the distribution of dark layers (Fig. 2) reveals that most biomarker content peaks occurred in the dark layers. The high contents of brassicasterol, dinosterol and TOC in MIS 2 within a particularly thick (>40 cm thick) dark layer were a result of better preservation under bottom water anoxic conditions, indicated by fine lamination, high values of the  $S_{pyrite}/C_{org}$  ratio, the absence of benthic foraminifera, and low values of the Re/Mo ratio (Oba et al., 1991; Tada et al., 1999; Watanabe et al., 2007). Some high biomarker contents in thinner dark layers during MIS 3 and MIS 4 were mostly the result of enhanced productivity, as preservation likely decreased under conditions of increasing oxygenation of bottom water (Watanabe et al., 2007). The highest TOC and biomarker contents occurred in dark layers of MIS 5, most likely caused by very high productivity as preservation was likely poor as the JS was very well ventilated (Tada et al., 1999; Watanabe et al., 2007; Yokoyama et al., 2007). On the other hand, biomarker and TOC contents were not always lower in light layers, for example, brassicasterol and dinosterol peaks occurred in light layers during MIS 5 (ca 95 ka) and MIS 3 (ca 45–50 ka). These differences suggest that sedimentary environmental conditions could affect biomarkers and TOC differently. Overall, the glacial-interglacial differences in TOC and biomarker contents in the JS have been smoothed since a higher portion of OM was degraded during the high productivity interglacials while a higher portion of OM was preserved during the low productivity glacials.

### 3.2. Normalized biomarker content and phytoplankton community structure

Plotted in Fig. 3 are the normalized contents of the diatom (Fig. 3B), dinoflagellate (Fig. 3C) and coccolithophorid (Fig. 3D) biomarkers, as indicators of their relative contributions to total phytoplankton productivity. Also shown are the *n*-alkanol content (TOM Fig. 3E) as an indicator of terrestrial input, and the percentage of *Parlia sulcata* (Fig. 3F) as an indicator of low salinity water mass flow to the JS (Tada et al., 1999). Although there are millennial scale oscillations, the most noticeable features of the normalized biomarker content records are the clear glacial-interglacial contrasts among the individual phytoplankton contributions. Coccolithophorid contribution was much lower during MIS 6 and 2 than during MIS 5, 4, 3 and 1, while diatom and dinoflagellate contributions showed the opposite trends. Thus, our biomarker records suggest major changes in community structure on a glacial-interglacial timescale, with peak glacials characterized by a more siliceous community and the interglacials characterized by a more calcareous community.

Several types of environmental change could have caused community structure changes in the JS. Firstly, phytoplankton community structure change is related to nutrient input and total productivity changes. In modern oceans, coccolithophorids are favored in high temperature, lower nutrient environments (Chen et al., 2007; Falkowski and Oliver, 2007) while diatoms thrive in high nutrient environments, especially those with high dissolved silicon concentrations (Egge and Aksnes, 1992), as coccolithophorids can out-compete dinoflagellates and diatoms under low nutrient environmental conditions due to smaller cell sizes and larger specific surface areas. Our biomarker content records and results of earlier studies all suggest lower nutrient input and lower productivity during peak glacials in the JS, which would normally have resulted in relatively more coccolithophorid contributions,

but our records suggest the opposite shift. Thus nutrient input and productivity changes were not the likely causes of glacial-interglacial timescale community structure changes in the JS.

Since bicarbonate ions are used in the formation of coccolithophorid shells, salinity (hence bicarbonate ion) changes can affect coccolithophorid growth and alter phytoplankton community structure. For example, alkenone content was shown to decrease between a fjord and a freshened isolated lake in Norway (Innes et al., 1998), likely in response to salinity changes. *E. huxleyi*, generally the major coccolithophorid species in open ocean and marginal seas, has not been reported in seawater with salinities below 11 psu (Bukry et al., 1970; van der Meer et al., 2008). In the ECS with a large salinity gradient from the coast to the open ocean, coccolithophorid fossils were rarely found in sediments from the coast to the 50 m bathymetric line, but they were common in deeper water sediments (Wang and Chen, 1988). In the Yellow Sea (YS), alkenone content is very low in surface sediments near the coast, but it is much higher in sediments further off the coast (Zhao and Xing et al., unpublished data). One explanation for these patterns is that lower salinity near the coast limited coccolithophorid growth in the ECS and YS.

Thus, lower coccolithophorid productivity in the JS during the glacials could be caused by lower salinity. The influx of the saline TWC decreased significantly due to the lowering of sea level while the relative contribution of the low salinity ECSCW increased due to the proximity of the Changjiang and Huanghe river mouths to the Tsushima Strait (Fig. 1), both would have resulted in low salinity conditions in the JS. Several lines of evidence provide support for these inferences: increased abundance of coastal water-dwelling diatom species *P. sulcata* (Fig. 3F) during the LGM (Ryu et al., 2005; Yokoyama et al., 2007), increased *n*-alkanol (Fig. 3E) content during the glacials. Our *n*-alkanol records are consistent with previous results, for example, increased terrestrial organic matter inputs during glacial maxima were inferred from the measurement of  $\delta^{13}C$  and  $\delta^{15}N$  of organic matter (Khim et al., 2007) and from the increased content of long chain *n*-alkanes (Ishiwatari et al., 1994). The relative abundance of the  $C_{34:2}EE$  alkenone was found to be sensitive to salinity (Fujine et al., 2006) and its increased abundance during the glacials suggested fresher surface conditions (Fujine et al., 2006, 2009). Planktonic foraminiferal  $\delta^{18}O$  values in the JS during the glacials were much lighter than the Holocene values (Fig. 3G), a unique isotopic anomaly which has been attributed to lower salinity during the glacials (Ikeda et al., 1999; Gorbarenko and Southon, 2000; Khim et al., 2007; Kido et al., 2007; Lee, 2007; Yokoyama et al., 2007). Salinity reconstruction using planktonic foraminiferal  $\delta^{18}O$  and alkenone temperature suggests that the JS surface salinity between 14 and 15 ka was 12 psu lower than that of today, and it was 15–18 psu lower during the glacial period than today assuming a cooling of 3 °C for the glacial period (Lee, 2007).

Therefore, a low-salinity environment during glacial period resulted in much lower calcareous plankton productivity which caused the shift of the dominant phytoplankton species to more siliceous in the JS, in spite of lower nutrient supplies and lower productivity. During the interglacials, the inflow of the TWC into the JS significantly increased the surface salinity which increased the relative contribution of coccolithophorids to total productivity even though total productivity also increased.

### 3.3. Comparison of biomarker and other community structure proxy records

Our biomarker-reconstructed community structure shift on a glacial-interglacial timescale is in contrast to the pattern indicated by published BSi and carbonate records from the JS (Oba et al.,

1991; Hyun et al., 2007; Kido et al., 2007), although most of the previous records only span the LGM to Holocene transition. The difference could be related to the robustness of the community structure proxies, and a direct comparison of all available records from the same site (ODP Site 797) may offer some insight. The BSi record (Fig. 4A) reveals a clear glacial-interglacial pattern with values for the interglacial stages (MIS 5, 3 and 1) much higher than those for the glacial stages (MIS 6, 4 and 2), consistent with results from other cores (Oba et al., 1991; Hyun et al., 2007; Kido et al., 2007). Carbonate values for the LGM and Termination I were much higher than Holocene values, but the average MIS 6 values were much lower than average MIS 5 values (Fig. 4B), thus a consistent glacial-interglacial pattern does not emerge. As diatom productivity proxies, brassicasterol content and BSi percentage have no correlations (Fig. 4A), and major differences between these two proxies occurred during MIS 5e and the Holocene, where very low brassicasterol contents were coeval with broad BSi peaks. As calcareous phytoplankton indicators, alkenone and carbonate contents have poor correlations (Fig. 4B). High contents for both alkenones and carbonate occurred only during early MIS 5, but the higher alkenone values in MIS 5a and 5c correlated with low carbonate contents.

Using the Ca/BSi ratio as a phytoplankton community proxy, previous studies suggested a more calcareous community during the LGM and a more siliceous community during the Holocene in the JS (Hyun et al., 2007). Higher Ca/BSi ratios in ODP Site 797 (Fig. 4C) during the LGM and Termination I than during the Holocene indeed suggest a more calcareous community during the LGM, however except for a small peak, very low Ca/BSi ratios during MIS 6 and the PGM (Fig. 4C) indicate no shift to a more calcareous community. Thus, the ODP Site 797 Ca/BSi ratio record does not reveal a consistent glacial-interglacial pattern of community structure change. The alkenone/brassicasterol ratio has been used as a phytoplankton community proxy (Werne et al., 2000; Higgsinon and Altabet, 2004), and this ratio in ODP Site 797 (Fig. 4D) reveals a clear glacial-interglacial pattern over the last two climate cycles, suggesting a more calcareous community during the interglacials and a more siliceous community during the glacials. Therefore, major differences exist between JS glacial-interglacial community structure changes revealed by the Ca/BSi ratio and our biomarker ratio. One possible reason for the differences is that alkenones can be produced by noncalcifying species (such as *Isochrysis galbana* and *Chrysothila lamellose*) in coastal regions (Theroux et al., 2010, and references herein). As the JS salinity decreased significantly during the glacials (Lee, 2007), coastal noncalcifying species would be more abundant and biogenic carbonate would be less abundant, but the Site 797 record reveals more biogenic carbonate deposition during the glacials. Thus, it is unlikely that coccolithophorid species changes caused the differences between the biomarker and the Ca/BSi ratios. However, as discussed in Section 3.1, coccolithophorids are also producers of brassicasterol, uncertainties remain for the use of the alkenone/brassicasterol ratios as a coccolithophorid-diatom proxy.

Another possible reason for the discrepancies is the additional sources for BSi and carbonate, such as radiolarians' contributions to BSi during interglacials (Itaki et al., 2007) and foraminifers' contributions to BCa. Peak values of BCa in core TY99PC18 from the JS during MIS 2 were initially attributed to enhanced foraminifer flux (Lee et al., 2003), but this was found to be unlikely since foraminiferal fossils were rare during glacial periods (Tada et al., 1999).

A more likely reason could be related to the different environmental controls on BSi and CaCO<sub>3</sub> dissolution/preservation. BSi dissolution is controlled by a variety of factors including the degree of undersaturation, pH, temperature, specific surface areas, organic

coating and Al/Si ratio (Ragueneau et al., 2000; Van Cappellen et al., 2002). BSi specific dissolution rates are much higher in the surface ocean than in the deep ocean and in sediments, resulting in 10–100% of the BSi dissolved in the euphotic zones (Van Cappellen et al., 2002, and references herein). A higher proportion of BSi production during diatom blooms can be exported and buried in sediments, while BSi production during non-bloom periods is mostly recycled in the euphotic zone (Brzezinski et al., 2003). Thus, although diatom blooms typically occur for only a short period of time, these blooms could account for a large fraction of the annual BSi export and burial (Brzezinski et al., 2003). For ODP Site 797, sedimentary BSi peaks during interglacials reflected not only higher BSi production, but also a higher proportion of BSi buried in sediments. During the glacials, most BSi production would have been dissolved, thus sedimentary BSi could not accurately reflect productivity changes.

Carbonate dissolution in the ocean is mostly controlled by pH (dissolved CO<sub>2</sub>) and temperature, and occurs mainly in the deep ocean. It has been suggested that high carbonate content during the LGM in the JS was mostly due to better preservation since lower productivity and lower organic matter export resulted in lower deep water CO<sub>2</sub> concentration (Lee et al., 2000). Thus, the carbonate peaks in Site 797 during the LGM and Termination I were also likely the result of enhanced preservation. But, MIS 6 carbonate was very low, suggesting more carbonate dissolution compared with the LGM. Low carbonate contents in ODP Site 797 during early MIS 5 and mid-late Holocene were most likely caused by strong dissolution as the increased productivity would have increased deep water CO<sub>2</sub>. Lee et al. (2003) also observed high productivity and low carbonate content during the early Holocene in core TY99PC18 from the southern JS, and concluded that although CaCO<sub>3</sub> production was high it was almost completely dissolved in the water column. Therefore, carbonate contents in the JS mostly reflected the dissolution effect.

Based on the above discussions, it is most likely that higher Ca/BSi ratios during the LGM and Termination I reflected better preservation of carbonate instead of increased calcareous production; while lower Ca/BSi ratios during early MIS5 and the Holocene were from a combined effect of higher diatom production, better BSi preservation, and increased CaCO<sub>3</sub> dissolution. We, therefore, suggest that Ca/BSi ratios in the JS sediments are not always a reliable proxy for phytoplankton community structure.

The degradation of biomarkers is mostly controlled by bottom water oxygen level in the JS, for example, we have concluded that lower brassicasterol (Fig. 4A), and alkenone (Fig. 4B) contents during MIS 5e and the Holocene were caused by strong oxic degradation when bottom water oxygen was high (Fig. 4F). Nevertheless, the degradation of different biomarkers is controlled by similar environmental conditions, thus sedimentary contents of different biomarkers can be evaluated comparatively. In our study, we have selected biomarkers which have been suggested to have similar chemical properties and degradation rates (Hinrichs et al., 1999), thus their ratios are less affected by degradation and have been successfully used as phytoplankton community structure proxies (Schubert et al., 1998; Werne et al., 2000; Higgsinon and Altabet, 2004; Zhao et al., 2006; Xing et al., 2008). However, it has also been reported that brassicasterol could be more sensitive to oxidation than alkenones (Sinninghe Damsté et al., 2002), potentially limiting the use of these biomarker ratios. The effect of oxidation on biomarker ratios can be partially evaluated using the alcohol index (the C<sub>26</sub> *n*-alcohol/C<sub>29</sub> *n*-alkane ratio). Since C<sub>26</sub> *n*-alcohol is less stable than C<sub>29</sub> *n*-alkane, the alcohol index would decrease as environmental conditions become more oxic, and vice versa (Cacho et al., 2000; Martrat et al., 2007). In Site 797, the alcohol index oscillated between 0.8 and 5.5 without an obvious

interglacial-glacial trend (Fig. 4G). The alcohol index and the bottom water oxygen level (Fig. 4F) reveals some similarities, for example, during the early MIS 5e and the mid-late Holocene. However, there are also major differences, for example, the MIS 6 suboxic conditions correlated with lower alcohol index values. These results suggest that input ratios of C<sub>26</sub> n-alcohol/C<sub>29</sub> n-alkane probably also oscillated, in addition to alterations by changes in environmental conditions. The alkenone/brassicasterol ratios do not correlate well with the alcohol index (Fig. 4G) or the bottom water oxygen levels (Fig. 4F), suggesting that, even though being modified by oxidic degradation, the alkenone/brassicasterol ratios mainly reflected community structure changes in the surface water.

Based on biomarker results, which need to be further confirmed, a preliminary conclusion can be made that the JS glacial

productivity was lower with greater contributions from siliceous phytoplankton while interglacial productivity was higher with greater contributions from calcareous phytoplankton. Our biomarker records afford a modification of the schemes proposed by Tada et al. (1999) and Hyun et al. (2007) to describe the circulation, phytoplankton productivity and community structure, redox and sediment biomarker content changes controlled mostly by sea-level changes in the JS (Fig. 5):

Mode I: sea level < -90 m, MIS 2 and MIS 6. With very limited TWC and ECSCW flow, nutrient inputs were low from the ECS; lowest surface salinity resulted in strong stratification and further reduced nutrients from deep water; these conditions resulted in the lowest productivity of the last 166 kyr and the lowest coccolithophorid/diatom ratios; the lowest dissolved oxygen (DO)

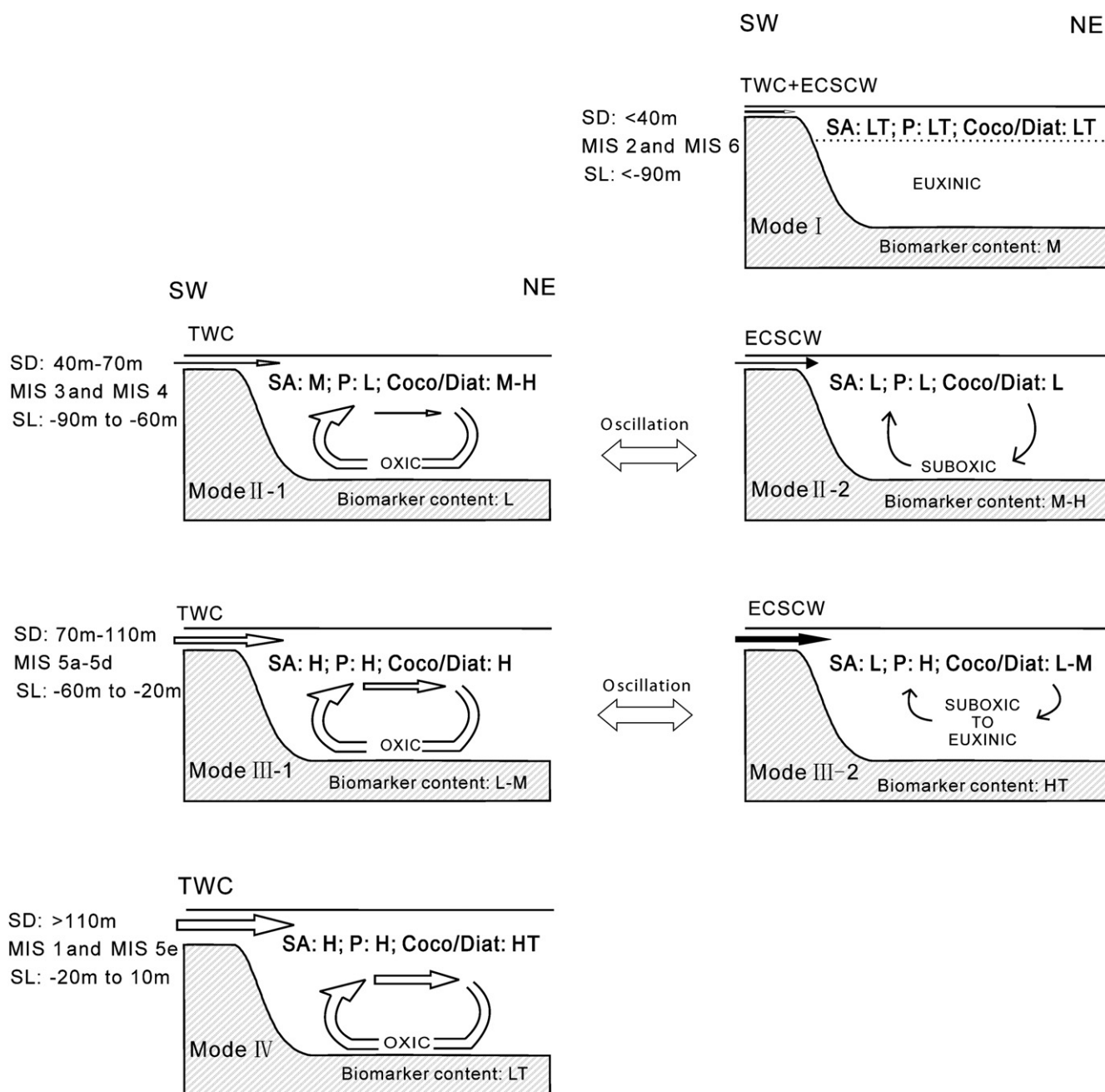


Fig. 5. A scheme illustrating the four modes of circulation in the Japan Sea and the associated environmental and ecosystem changes, modified from Tada et al. (1999) and Hyun et al. (2007). SA: surface salinity; P: productivity; Coco/diatom: coccolithophorid/diatom ratio; HT: highest; H: high; M: intermediate; L: low; LT: lowest; SD: the Tsushima Strait sill depth; SL: sea level; TWC: the Tsushima Warm Current; ECSCW: East China Sea coastal water.

concentration favored organic matter preservation, and resulted in intermediate TOC and biomarker contents in sediments.

Mode II-1: sea level, –90 m to –60 m; MIS 3 and 4, dry intervals. With increased TWC flow but almost no ECSCW flow, nutrient inputs were low from the ECS; intermediate surface salinity resulted in increased ventilation and increased nutrient availability from deep water; these conditions still resulted in low productivity and intermediate to high coccolithophorid/diatom ratios; high DO increased organic matter degradation, and resulted in low TOC and biomarker contents in sediments.

Mode II-2: sea level, –90 m to –60 m; MIS 3 and 4, wet intervals. With restricted TWC flow but increased ECSCW flow, nutrient inputs were high from the ECS; low surface salinity resulted in limited ventilation and decreased nutrient availability from deep water; these conditions still resulted in low productivity and low coccolithophorid/diatom ratios; intermediate DO increased organic matter preservation, and resulted in intermediate to high TOC and biomarker contents in sediments.

Mode III-1: sea level, –60 m to –20 m, MIS 5a–5d, dry intervals. With higher TWC flow but low ECSCW flow, nutrient inputs were low from the ECS; high surface salinity resulted in strong ventilation and increased nutrient availability from deep water; these conditions resulted in high productivity and high coccolithophorid/diatom ratios; high DO increased organic matter degradation, and resulted in low to intermediate TOC and biomarker contents in sediments.

Mode III-2: sea level, –60 m to –20 m, MIS 5a–5d, wet intervals. With low TWC flow but high ECSCW flow, nutrient inputs were high from the ECS; low surface salinity resulted in restricted ventilation and decreased nutrient availability from deep water; these conditions resulted in high productivity and low to intermediate coccolithophorid/diatom ratios; low DO increased organic matter preservation, and resulted in the highest TOC and biomarker contents in sediments.

Mode IV: sea level, –20 m to +10 m, early MIS 5e and mid-Holocene. With the highest TWC flow but low ECSCW, nutrient inputs were low from the ECS; high surface salinity resulted in strong ventilation and increased nutrient availability from deep water; these conditions resulted in high productivity and the highest coccolithophorid/diatom ratios; the highest DO increased organic matter degradation, and resulted in the lowest TOC and biomarker contents in sediments.

#### 4. Conclusions

Biomarker contents in the JS have reflected both productivity and bottom water redox conditions which resulted in high biomarker content values during both glacial and interglacial periods, and revealing no clear glacial-interglacial patterns.

Biomarker records provide additional evidence suggesting that glacial productivity was lower due to reduced nutrient input mainly as a result of water column stratification and reduced flow through the Tsushima Strait.

Factors governing BSi and CaCO<sub>3</sub> dissolution are different, so the use of the sedimentary Ca/BSi ratio as a phytoplankton community proxy can lead to ambiguous conclusions. Even though biomarkers have different stabilities, factors governing the oxic degradation of the selected biomarkers are similar, and their ratios in sediments have the potential to be useful phytoplankton community structure proxies.

In contrast to previous results based on Ca/BSi ratios, biomarker ratios reveal a shift from a diatom-dominated community during the glacials to a coccolithophorid-dominated community during the interglacials, mainly as a result of surface salinity changes in the JS controlled by sea-level changes.

#### Acknowledgments

We thank Hailong Zhang for technical assistance and the ODP for samples. This study was supported by the National Basic Research Program of China (973 Program 2010CB428901) and the National Natural Science Foundation of China (Grant No. 40976042, 40776029, 40431002, 41076038).

#### References

- Brzezinski, M.A., Jones, J.L., Bidle, K.D., Azam, F., 2003. The balance between silica production and silica dissolution in the sea: insights from Monterey Bay, California, applied to the global data set. *Limnol. Oceanogr.* 48 (5), 1846–1854.
- Bukry, D., King, S.A., Horn, M.K., Manheim, F.T., 1970. Geological significance of coccoliths in fine-grained carbonate bands of postglacial Black Sea sediments. *Nature* 226, 156–158.
- Cacho, I., Grimalt, J.O., Sierro, F.J., Shackleton, N., Canals, M., 2000. Evidence for enhanced Mediterranean thermohaline circulation during rapid climatic coolings. *Earth Planet Sci. Lett.* 183 (3–4), 417–429.
- Calvo, E., Pelejero, C., Logan, G.A., De Deckker, P., 2004. Dust-induced changes in phytoplankton composition in the Tasman Sea during the last four glacial cycles. *Paleoceanography* 19, 2020.
- Chen, Y.L., Chen, H.Y., Chung, C.W., 2007. Seasonal variability of coccolithophore abundance and assemblage in the northern South China Sea. *Deep Sea Res. Part II* 54 (14–15), 1617–1633.
- Dahl, K.A., Repeta, D.J., Goericke, R., 2004. Reconstructing the phytoplankton community of the Cariaco Basin during the Younger Dryas cold event using chlorin steryl esters. *Paleoceanography* 19 (1), 19–29.
- Sinninghe Damsté, J.S., Rijpstra, W.I.C., Reichert, G.J., 2002. The influence of oxic degradation on the sedimentary biomarker record II. Evidence from Arabian Sea sediments. *Geochim. Cosmochim. Acta* 66 (15), 2737–2754.
- Egge, J.K., Aksnes, D.L., 1992. Silicate as regulating nutrient in phytoplankton competition. *Mar. Ecol. Prog. Ser.* 83 (2–3), 281–289.
- Falkowski, P., Oliver, M., 2007. Mix and match: how climate selects phytoplankton. *Nat. Rev. Microbiol.* 5 (10), 813–819.
- Fujine, K., Yamamoto, M., Tada, R., Kido, Y., 2006. A salinity-related occurrence of a novel alkenone and alkenoate in late Pleistocene sediments from the Japan Sea. *Org. Geochem.* 37 (9), 1074–1084.
- Fujine, K., Tada, R., Yamamoto, M., 2009. Paleotemperature response to monsoon activity in the Japan Sea during the last 160 kyr. *Paleogeogr. Paleoclimatol. Paleoecol.* 280 (3–4), 350–360.
- Gorbarenko, S.A., 1996. Stable isotope and lithologic evidence of late-glacial and Holocene oceanography of the northwestern Pacific and its marginal seas. *Quaternary Res.* 46 (3), 230–250.
- Gorbarenko, S.A., Southon, J.R., 2000. Detailed Japan Sea paleoceanography during the last 25 kyr: constraints from AMS dating and  $\delta^{18}\text{O}$  of planktonic foraminifera. *Paleogeogr. Paleoclimatol. Paleoecol.* 156 (3–4), 177–193.
- Higginson, M.J., Altabet, M.A., 2004. Initial test of the silicic acid leakage hypothesis using sedimentary biomarkers. *Geophys. Res. Lett.* 31 (18), L18303.
- Hinrichs, K.U., Schneider, R.R., Mueller, P.J., Rullkoetter, J., 1999. A biomarker perspective on paleoproductivity variations in two late Quaternary sediment sections from the southeast Atlantic Ocean. *Org. Geochem.* 30 (5), 341–366.
- Hyun, S., Bahk, J.J., Suk, B.C., Park, B.K., 2007. Alternative modes of Quaternary pelagic biosiliceous and carbonate sedimentation: a perspective from the East Sea (Japan Sea). *Paleogeogr. Paleoclimatol. Paleoecol.* 247 (1–2), 88–99.
- Ijiri, A., Wang, L.J., Oba, T., Kawahata, H., Huang, C.Y., 2005. Paleoenvironmental changes in the northern area of the east China Sea during the past 42,000 years. *Paleogeogr. Paleoclimatol. Paleoecol.* 219 (3–4), 239–261.
- Ikeda, M., Suzuki, F., Oba, T., 1999. A box model of glacial-interglacial variability in the Japan Sea. *J. Oceanogr.* 55 (4), 483–492.
- Innes, H.E., Bishop, A.N., Fox, P.A., Head, I.M., Farrimond, P., 1998. Early diagenesis of bacteriohopanoids in recent sediments of Lake Pollen, Norway. *Org. Geochem.* 29 (5–7), 1285–1295.
- Irino, T., Tada, R., 2000. Quantification of aeolian dust (Kosa) contribution to the Japan Sea sediments and its variation during the last 200 ky. *Geochemical J.* 34 (1), 59–93.
- Irino, T., Tada, R., 2002. High-resolution reconstruction of variation in aeolian dust (Kosa) deposition at ODP site 797, the Japan Sea, during the last 200 ka. *Global Planet. Change* 35 (1–2), 143–156.
- Ishiwatari, R., Hirakawa, Y., Uzaki, M., Yamada, K., Yada, T., 1994. Organic geochemistry of the Japan Sea sediments; 1, bulk organic matter and hydrocarbon analyses of core KH-79-3, C-3 from the Oki Ridge for paleoenvironment assessments. *J. Oceanogr.* 50 (2), 179–195.
- Ishiwatari, R., Yamada, K., Matsumoto, K., Houtatsu, M., Naraoka, H., 1999. Organic molecular and carbon isotopic records of the Japan Sea over the past 30 kyr. *Paleoceanography* 14 (2), 260–270.
- Ishiwatari, R., Houtatsu, M., Okada, H., 2001. Alkenone-sea surface temperatures in the Japan Sea over the past 36 kyr: warm temperatures at the last glacial maximum. *Org. Geochem.* 32 (1), 57–67.
- Itaki, T., Komatsu, N., Motoyama, I., 2007. Orbital- and millennial-scale changes of radiolarian assemblages during the last 220 kyrs in the Japan Sea. *Paleogeogr. Paleoclimatol. Paleoecol.* 247 (1–2), 115–130.

- Khim, B.K., Bahk, J.J., Hyun, S., Lee, G.H., 2007. Late Pleistocene dark laminated mud layers from the Korea Plateau, western East Sea/Japan Sea, and their paleoceanographic implications. *Paleogeogr. Paleoclimatol. Paleoecol.* 247 (1–2), 74–87.
- Kido, Y., Minami, I., Tada, R., Fujine, K., Irino, T., Ikehara, K., Chun, J.H., 2007. Orbital-scale stratigraphy and high-resolution analysis of biogenic components and deep-water oxygenation conditions in the Japan Sea during the last 640 kyr. *Paleogeogr. Paleoclimatol. Paleoecol.* 247 (1–2), 32–49.
- Koizumi, I., Tada, R., Narita, H., Irino, T., Aramaki, T., Oba, T., Yamamoto, H., 2006. Paleocyanographic history around the Tsugaru Strait between the Japan Sea and the northwest Pacific Ocean since 30 cal kyr BP. *Paleogeogr. Paleoclimatol. Paleoecol.* 232 (1), 36–52.
- Lee, K.E., 2007. Surface water changes recorded in late Quaternary marine sediments of the Ulleung Basin, East Sea (Japan Sea). *Paleogeogr. Paleoclimatol. Paleoecol.* 247 (1–2), 18–31.
- Lee, G., Park, S., Kim, D., 2000. Fluctuations of the calcite compensation depth (CCD) in the East Sea (Sea of Japan). *Geo-Marine Lett.* 20 (1), 20–26.
- Lee, K., Bahk, J., Narita, H., 2003. Temporal variations in productivity and planktonic ecological structure in the East Sea (Japan Sea) since the last glaciation. *Geo-Marine Lett.* 23 (2), 125–129.
- Lee, K.E., Bahk, J.J., Choi, J., 2008. Alkenone temperature estimates for the East Sea during the last 190,000 years. *Org. Geochem.* 39 (6), 741–753.
- Müller, P.J., Kirst, G., Ruhland, G., von Storch, I., Rosell-Mele, A., 1998. Calibration of the alkenone paleotemperature index  $U_{37}^K$  based on core-tops from the eastern South Atlantic and the global ocean (60 degrees N–60 degrees S). *Geochim. Cosmochim. Acta* 62 (10), 1757–1772.
- Martrat, B., Grimalt, J., Shackleton, N., de Abreu, L., Hutterli, M., Stocker, T., 2007. Four climate cycles of recurring deep and surface water destabilizations on the Iberian margin. *Science* 317 (5837), 502–507.
- Menzel, D., van Bergen, P.F., Schouten, S., Sinninghe Damste, J.S., 2003. Reconstruction of changes in export productivity during Pliocene sapropel deposition; a biomarker approach. *Paleogeogr. Paleoclimatol. Paleoecol.* 190, 273–287.
- Oba, T., Kato, M., Kitazato, H., Koizumi, I., Omura, A., Sakai, T., Takayama, T., 1991. Paleoenvironmental changes in the Japan Sea during the last 85,000 years. *Paleoceanography* 6 (4), 499–518.
- Oba, T., Irino, T., Yamamoto, M., Murayama, M., Takamura, A., Aoki, K., 2006. Paleocyanographic change off central Japan since the last 144,000 years based on high-resolution oxygen and carbon isotope records. *Global Planet. Change* 53 (1–2), 5–20.
- Ohkushi, K., Itaki, T., Nemoto, N., 2003. Last Glacial-Holocene change in intermediate-water ventilation in the northwestern Pacific. *Quat. Sci. Rev.* 22 (14), 1477–1484.
- Ragueneau, O., Treguer, P., Leynaert, A., Anderson, R.F., Brzezinski, M.A., DeMaster, D.J., Dugdale, R.C., Dymond, J., Fischer, G., Francois, R., Heinze, C., Maier-Reimer, E., Martin-Jezequel, V., Nelson, D.M., Queguiner, B., 2000. A review of the Si cycle in the modern ocean: recent progress and missing gaps in the application of biogenic opal as a paleoproductivity proxy. *Global Planet. Change* 26 (4), 317–365.
- Ryu, E., Yi, S., Lee, S.J., 2005. Late Pleistocene-Holocene paleoenvironmental changes inferred from the diatom record of the Ulleung Basin, East Sea (Sea of Japan). *Mar. Micropaleontol.* 55 (3–4), 157–182.
- Schubert, C.J., Villanueva, J., Calvert, S.E., Cowie, G.L., von Rad, U., Schultz, H., Berner, U., Erlenkeuser, H., 1998. Stable phytoplankton community structure in the Arabian Sea over the past 200,000 years. *Nature* 394 (6693), 563–566.
- Schulte, S., Bard, E., 2003. Past changes in biologically mediated dissolution of calcite above the chemical lysocline recorded in Indian Ocean sediments. *Quat. Sci. Rev.* 22 (15–17), 1757–1770.
- Seki, O., Ikehara, M., Kawamura, K., Nakatsuka, T., Ohnishi, K., Wakatsuchi, M., Narita, H., Sakamoto, T., 2004. Reconstruction of paleoproductivity in the Sea of Okhotsk over the last 30 kyr. *Paleoceanography* 19 (1), 1016.
- Tada, R., Irino, T., Koizumi, I., 1999. Land-ocean linkages over orbital and millennial timescales recorded in late Quaternary sediments of the Japan Sea. *Paleoceanography* 14 (2), 236–247.
- Tada, R., Oba, T., Jordan, R.W., 2007. Preface for special volume: “Quaternary paleoceanography of the Japan Sea and its linkage with Asian monsoon”. *Paleogeogr. Paleoclimatol. Paleoecol.* 247 (1–2), 1–4.
- Theroux, S., D’Andrea, W.J., Toney, J., Amaral-Zettler, L., Huang, Y., 2010. Phylogenetic diversity and evolutionary relatedness of alkenone-producing haptophyte algae in lakes: implications for continental paleotemperature reconstructions. *Earth Planet Sci. Lett.* 300 (3–4), 311–320.
- Van Cappellen, P., Dixit, S., van Beusekom, J., 2002. Biogenic silica dissolution in the oceans: reconciling experimental and field-based dissolution rates. *Global Biogeochem. Cycles* 16 (4), 1075.
- van der Meer, M.T.J., Sangiorgi, F., Baas, M., Brinkhuis, H., Sinninghe Damste, J.S., Schouten, S., 2008. Molecular isotopic and dinoflagellate evidence for late Holocene freshening of the Black Sea. *Earth Planet Sci. Lett.* 267 (3–4), 426–434.
- Volkman, J., 1986. A review of sterol markers for marine and terrigenous organic matter. *Org. Geochem.* 9 (2), 83–99.
- Waelbroeck, C., Labeyrie, L., Michel, E., Duplessy, J.C., McManus, J.F., Lambeck, K., Balbon, E., Labracherie, M., 2002. Sea-level and deep water temperature changes derived from benthic foraminifera isotopic records. *Quat. Sci. Rev.* 21 (1–3), 295–305.
- Wang, P., Chen, X., 1988. The distribution of calcareous nannofossil from the surface sediments in the east China Sea. *Acta Oceanol. Sin.* 10 (1), 76–85 (in Chinese).
- Watanabe, S., Tada, R., Ikehara, K., Fujine, K., Kido, Y., 2007. Sediment fabrics, oxygenation history, and circulation modes of Japan Sea during the Late Quaternary. *Paleogeogr. Paleoclimatol. Paleoecol.* 247 (1–2), 50–64.
- Werne, J.P., Hollander, D.J., Lyons, T.W., Peterson, L.C., 2000. Climate-induced variations in productivity and planktonic ecosystem structure from the Younger Dryas to Holocene in the Cariaco Basin, Venezuela. *Paleoceanography* 15 (1), 19–29.
- Winter, A., Jordan, R.W., Roth, P.H., 1994. Biogeography of living coccolithophores in ocean waters. In: Winter, A., Siesser, W.S. (Eds.), *Coccolithophores*. Cambridge University Press, pp. 161–177.
- Xing, L., Zhao, M., Zhang, H., Liu, Y., Shi, X., 2008. Biomarker reconstruction of phytoplankton productivity and community structure changes in the middle Okinawa Trough during the last 15 ka. *Chin. Sci. Bull.* 53 (16), 2552–2559.
- Yamada, K., Ishizaka, J., Nagata, H., 2005. Spatial and temporal variability of satellite primary production in the Japan Sea from 1998 to 2002. *J. Oceanogr.* 61 (5), 857–869.
- Yanagi, T., 2002. Water, salt, phosphorus and nitrogen budgets of the Japan Sea. *J. Oceanogr.* 58 (6), 797–804.
- Yokoyama, Y., Kido, Y., Tada, R., Minami, I., Finkel, R.C., Matsuzaki, H., 2007. Japan Sea oxygen isotope stratigraphy and global sea-level changes for the last 50,000 years recorded in sediment cores from the Oki Ridge. *Paleogeogr. Paleoclimatol. Paleoecol.* 247 (1–2), 5–17.
- Zhao, M.X., Mercer, J.L., Eglinton, G., Higginson, M.J., Huang, C.Y., 2006. Comparative molecular biomarker assessment of phytoplankton paleoproductivity for the last 160 kyr off Cap Blanc, NW Africa. *Org. Geochem.* 37 (1), 72–97.